Diode-laser-pumped, cw, Intracavity-doubled Nd:YLF Laser

Glen A. Rines, Richard A. Schwarz and Peter F. Moulton

Schwartz Electro-Optics, Inc.
Research Division
45 Winthrop Street
Concord, MA 01742

(508) 371-2299

Abstract

In this paper we describe the design and performance characteristics of a diode-laser-pumped, cw, Nd:YLF laser with intracavity second harmonic generation (SHG). We include descriptions of the micro-optics used to couple pump power from a 10-W diode laser to the Nd:YLF crystal in an end-pumped configuration; the opto-mechanical design of the Nd:YLF gain element; the performance of the Nd:YLF laser at 1047 nm; and the design and performance of resonators configured for intracavity SHG with both KTP (II) and LBO (I) crystals. The highest output power obtained to date, with an LBO SHG crystal, was 1.25 W at 523.5 nm.

Introduction

The goal of this project was the development of an all-solid-state, cw, nominal 1-W green laser for pumping a cw titanium-sapphire laser. Our design approach was based on longitudinal pumping of Nd:YLF (operating at 1047 nm) with a 10-W cw diode laser array. Intracavity SHG was employed to generate output at 523.5 nm. The sections that follow describe the configuration of the pump optics, the laser performance at 1047 nm, and the SHG performance at 523.5 nm. We also report initial results obtained using the cw green laser to pump a cw titanium-sapphire laser.

Pumping Configuration

Practical use of a linear, diode-laser array to end-pump a laser crystal requires focusing the highly asymmetric output beam of the diode laser into a nominally circular cross section over the absorption length of the gain medium. In addition, it is desirable to minimize losses in the coupling optics to maximize the overall efficiency of the laser system. The diode laser used in these experiments is a 10-W “bar” with twelve emitting junctions in a 1-cm-long, monolithic array, each 1 x 200 μm in size and spaced at 800 μm (center-to-center). The output beam from these junctions is asymmetric in divergence as well as cross section. In the plane parallel to the 1-μm dimension the beam is close to diffraction limited with a divergence angle of approximately 35 degrees (FWHM). In the 200-μm dimension the beam is highly multimode with a divergence of around 10 degrees (FWHM).

Our design goal for the diode-laser coupling optics was to produce a pump beam well-matched to a TEM_{00} mode of 1-mm diameter in a 5-mm-long Nd:YLF crystal. Through a combination of modeling and experimentation we developed the micro-optics system shown in Fig. 1. A fast, short-focal-length cylinder lens is used to efficiently collect and nominally collimate the beam in the diffraction-limited plane. A microlens array is used to collect and collimate the beam in the non-diffraction-limited plane. Following the microlens we use a single-element, aspheric lens to focus the collimated diode-laser beam into the Nd:YLF crystal. All of these elements are anti-reflection coated at the diode-laser wavelength, 797 nm. The significant design features of these optical elements are described briefly below.

The collection lens, fabricated from a 2-mm diameter rod, has a hemispherical cross section and a focal length of 1.8 mm. When placed approximately

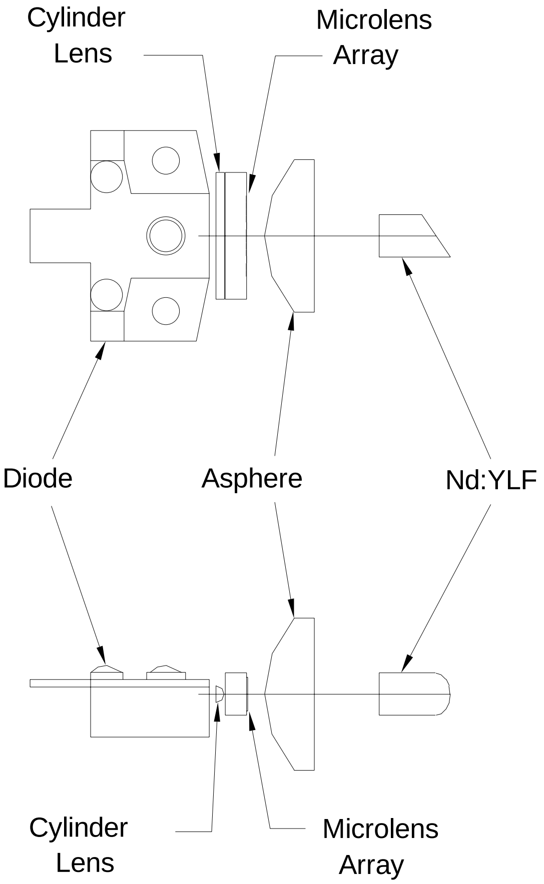

Figure 1. Pump optics layout.

1 mm from the diode junction, this lens collects the diode emission with 84% efficiency and yields a slightly divergent beam in the diffraction-limited plane. This beam, when subsequently focused by the asphere, yields the desired pumped volume in the Nd:YLF.

The microlens array consists of twelve cylinder lenses fabricated on a BK-7 glass substrate. The individual cylinder-lens elements are 800-μm wide and 4 mm long, with a focal length of approximately 3 mm. They are located at the plane where the beams from the individual emitters of the diode laser fill the lens aperture in the 800-μm dimension. The microlens array is placed to yield the best collimation of the diode-laser beam in the 800-μm dimension.

The focusing lens is a 12-mm-focal-length asphere. This lens focuses the pump beam into the Nd:YLF laser crystal. The measured beam profile was found to be in good agreement with the predictions of our ray-tracing model: 1.4-mm $1/e^2$ diameter at the focus, with the beam rapidly diverging in the horizontal plane and slightly converging in the vertical plane.

In the course of these experiments we evaluated both flat/flat and flat/Brewster Nd:YLF crystals. While the pump beam has a circular profile at the waist, the rapidly diverging beam in the horizontal plane leads to an elliptical gain profile in the 5-mm-long Nd:YLF crystal. We chose the flat/Brewster geometry because the single Brewster end provides two very desirable properties: a low loss interface for the π-polarized laser mode and an intrinsic anamorphic prism, which converts the elliptical pumped volume to a circularly symmetric mode in the laser resonator.

The gain element geometry chosen for the intracavity SHG experiments is a 4-mm-diameter, 5-mm-long, Brewster-cut, Nd:YLF crystal oriented with the c-axis parallel to both the pump polarization and the laser polarization. This selects the high-gain, 1047-nm laser transition in Nd:YLF and orients the diode-laser pump beam to be polarized for maximum absorption at 797 nm. The flat end of the crystal is coated for high transmission (98%T) at 797 nm and high reflection at 1047 nm. The crystal is conductively cooled by mounting it in a water-cooled, copper heat sink with a thermally conductive adhesive. The heat sink is designed to provide low-stress, but rigid, mounting and to maintain cylindrical symmetry for the stress and temperature paths between the crystal and the heat sink.

Laser Performance at 1047 nm

With the diode-laser pumping configuration and the Nd:YLF gain element described above, we conducted a series of standing-wave resonator experiments to evaluate the thermal, thermo-optic and opto-mechanical characteristics of the gain module. With a simple standing-wave resonator comprised of a 4-m-concave output coupler (95%R) and the Nd:YLF crystal, we obtained 3.85 W at 1047 nm with 10 W delivered to the face of the Nd:YLF crystal. The output beam was multimode and astigmatic. The input/output data are shown in Fig. 2. Data obtained using a cw titanium-sapphire laser as a pump source are shown for comparison with the diode-pumping results.

In addition to the multimode 1047-nm laser data, we made careful measurements of the thermal lens induced in the Nd:YLF crystal as a function of pump power. The thermal lensing data were needed to allow proper design of an efficient TEM_{00}-mode resonator.

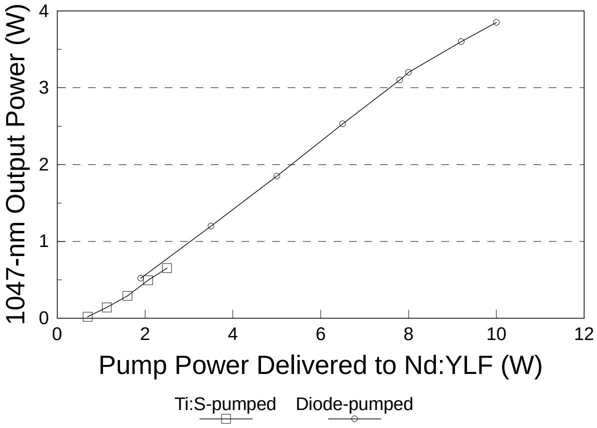

Figure 2. Laser performance at 1047 nm.

With 10 W delivered to the Nd:YLF, the crystal acted as a positive lens for π-polarized light with a focal length of 40 cm in the horizontal plane (parallel to the c-axis) and a 100-cm focal length in the orthogonal plane. End face curvature contributed significantly to the measured thermal lensing.

We experimented with a number of standing-wave and ring resonators. In these experiments we validated the design procedure and the accuracy of our thermal lensing data. We were able to construct resonators with the astigmatic thermal lens fully compensated, yielding circularly symmetric, near diffraction-limited, TEM_{00}-mode output beams. The highest power, TEM_{00}-mode output for 10 W of pump was 3.0 W at 1047 nm. This beam was symmetric and had a measured M^2 value of 1.2.

SHG Results

Having validated the design procedures, the integrity of the gain element at high pump powers, and the thermal lensing data, we designed a resonator configured for SHG, as shown in Fig. 3. This resonator compensates the astigmatic thermal lens with the two convex cylindrical mirrors shown. The TEM_{00} mode volume inside the Nd:YLF crystal is approximately 1.6 x 1.0 mm and, thus, is well-matched to the pumped volume. The intracavity SHG crystal is located at the beam waist (~80-μm diameter) produced by the two lenses. The dichroic high reflector completes the standing-wave cavity, reflecting both the fundamental and the harmonic waves. The SHG output is obtained in a single beam as shown in the figure.

We experimented with intracavity frequency-doubling using both KTP (Type II, 3x3x5 mm) and LBO (Type I, 3x3x15 mm). At the second harmonic wavelength, 523.5 nm, we obtained 304 mW using KTP, and 900 mW using LBO. Input/output data are shown in Fig. 4 for the LBO case. It should be noted that the lower output obtained using KTP was not due to a lower SHG conversion efficiency. The two crystals displayed roughly similar conversion efficiencies. However, extra intracavity components were required for polarization control in the Type II KTP case, leading to a lower circulating power at the fundamental wavelength.

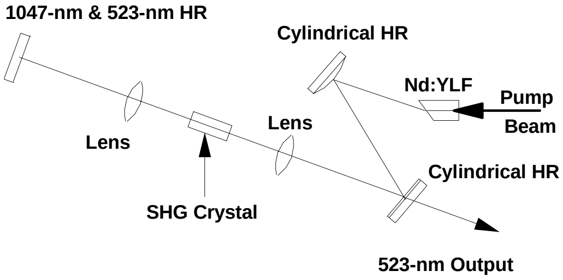

Figure 3. Resonator layout with intracavity SHG.

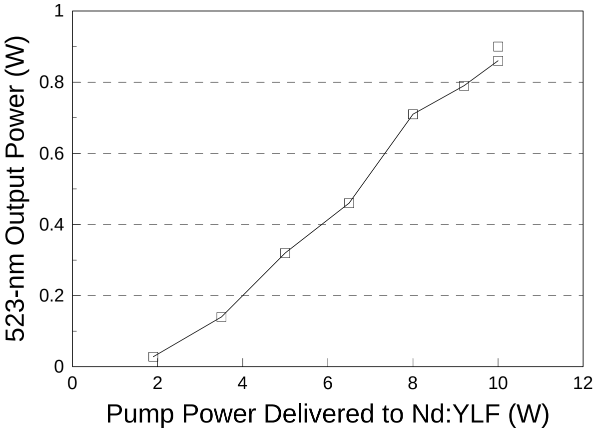

Figure 4. Laser performance at 523.5 nm using LBO.

We evaluated the performance characteristics of the laser shown in Fig. 3 and found that it suffered from mediocre beam quality and considerable high-frequency intensity noise. We accordingly made a number of modifications to the resonator that resulted in higher total output power, improved beam quality, and reduced intensity noise. We altered the resonator design so that only one cylindrical HR was required, instead of two, to compensate for the asymmetric thermal lensing. The lens and HR mirror shown to the left of the SHG crystal in Fig. 3 were replaced with a 5-cm, concave mirror. The mirror was located such that it produced the same cavity mode size as the lens/flat mirror combination. This mirror was highly reflective for 1047-nm and highly transmissive for the 523.5-nm SHG beam, resulting in two green output beams from the laser.

The modified resonator configuration is shown in Fig. 5. In this configuration we obtained 1.25 W of total output at 523.5 nm, in two beams. Mode quality was measured and characterized in terms of M^2 values in the x (horizontal) and y (vertical) planes. In the previous configuration, values of $M_x^2 = 1.8$ and $M_y^2 = 3.4$ had been measured. In the dual-output configuration, we obtained values of $M_x^2 = 1.2$ and $M_y^2 = 1.6$. A near-field output profile of the 523.5-nm beam appears in Figure 6.

We measured the intensity noise in the fundamental and SHG output beams under various operating conditions. In configurations which allowed feedback of the SHG output to the SHG crystal, the laser displayed chaotic high-frequency intensity noise. In the 1-beam SHG output configuration shown in Fig. 3, the laser displayed severe intensity noise, greater than 30% rms in the 0 - 1 MHz frequency band. (The average power, however, was stable.) The 2-beam SHG output configuration shown in Fig. 5 was much quieter. The noise was further reduced by angle-tuning the SHG crystal a few degrees off normal incidence, reducing feedback from the SHG crystal surfaces. In the dual-beam configuration we were able to reduce the high-frequency intensity noise in the SHG output to 2-3% rms. This was approximately the same noise level as that measured in the fundamental laser output in the absence of SHG.

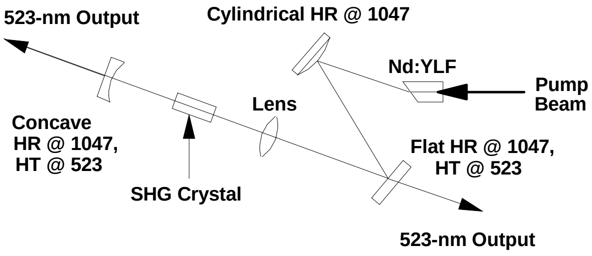

Figure 5. Dual-output resonator layout.

Figure 6. Near-field 523.5-nm output profile.

All-solid-state cw Ti:sapphire Laser Demonstration

We used the all-solid-state cw green laser to pump a cw, single-frequency, ring titanium-sapphire laser. The cw green laser was operating in its single-output configuration at a power level of 850 mW. The titanium-sapphire laser was equipped with a galvanometer-driven birefringent tuner for rapid wavelength tuning. The results are shown in Fig. 7. We obtained up to 16.5 mW of single-frequency, cw output from the titanium-sapphire laser. The output was rapidly tunable over a 120-nm wavelength region from 788 to 908 nm. The tuning range was limited on the short-wavelength end by the mirror coatings. Further improvements in performance are likely to be achieved with careful mode-matching of the pump beam to the titanium-sapphire resonator mode.

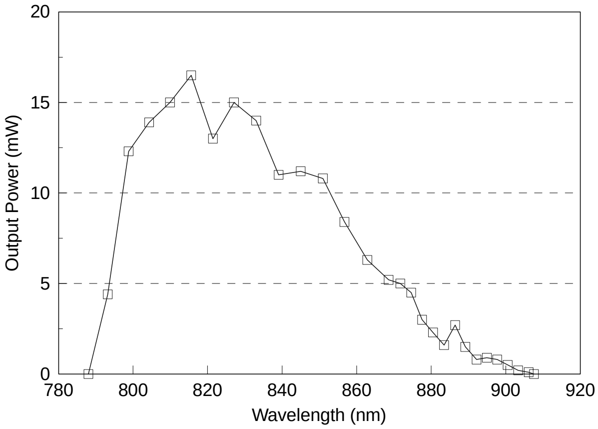

Figure 7. Tuning curve for the single-frequency cw titanium-sapphire laser pumped by the cw green laser. The pump power level is 850 mW.

Acknowledgments

This research was supported by NASA Langley Research Center. Additional funding was provided by E.I. du Pont de Nemours & Co.